CHAPTER 4

4.1 METHODOLOGY FOLLOWED FOR STRUCTURAL ANALYSIS

4.2 LINEAMENT MAPPING THROUGH GIS

4.3 FIELD STRUCTURES

4.4 STRUCTURAL SYNTHESIS

Chapter-4

Structural Analysis

The granitoid rocks of the study area present a polyphase deformation history. According to Das *et al*. (2018), the granitoids suffered five (D1-D5) structure-forming events as exemplified by interrelations of styles and orientations of various structural elements preserved within the deformed body. The five deformation events have been documented as follows:

(1) Poorly preserved D1-D2 structures formed in an end-Archaean transpressive deformation event resulting from oblique convergence of EDC with WDC at ca. 2.51 Ga and are mostly represented by NW-SE trending gneissic layering (S1), foliation (S2) and fold (F1-F2) structures.

(2) Mesoscopic conjugate shear zone development resulting from NW-SE strike parallel compression – D3.

(3) Later two successive brittle events marked by mesoscopic conjugate fracture development in granitoids (D4) and faulting and fracturing of granitoid-gneissic rocks along with overlying Srisailam Formation rocks (D5) respectively.

In the present study, both mesoscopic and large scale structural analyses were attempted to understand the role of brittle fracturing behind uranium mineralization. For mesoscopic structural analysis, systematic data collection regarding nature and orientation of D4-D5 stage fracture sets were done over the different mineralized blocks in the entire study area. Large scale structural analysis, on the other hand, was performed though analysis of lineament data from satellite imageries with the help of standard remote sensing software's as detailed below.

4.1 Methodology followed for structural analysis

Large – scale structural analysis involves lineament extraction from satellite images manually. In this method, the lineaments were extracted by image processing techniques. Usually, the lineaments appear on satellite images as straight lines or edges, this is contributed by the tonal differences within the surface material. The data used in this study are of IRSP6 LISS III imagery data downloaded from the USGS website. During this study ARC GIS 10.1 software package was used with geostatistical and geospatial tools to achieve the purpose of the study. Alongside, digital lineament maps were prepared following standard remote sensing techniques in the GIS platform using imagery data and Digital Elevation Mapping data downloaded from USGS website. Using geostatistical tool as an add-on tool within ARC GIS platform, histograms were drawn from the digital lineament map. Rose diagrams in the GIS platform were prepared using

polar plot and data from different blocks as established by AMD and mentioned earlier.

Mesoscopic structural analysis involves systematic measurement of fracture orientation data and count of fracture density in 2m x 2m grid pattern around the mineralized 'Main Block' and other adjoining blocks. This attempt has been made in the present study to estimate variation in fracture density within the basement granitoid with respect to increasing distance from the mineralized 'Main Block' in the Chitrial outlier.

4.2 Lineament mapping through GIS

Remote Sensing data are being used in solving various issues by digital image processing in a GIS platform. Detection of the geological linear features contributes significantly towards understanding of the structural scenario of an area. The term lineament/fracture is used to represent linear discontinuity in the basement rock produced as a result of tectonic phenomena. It may be a joint or a fracture or a fault or a trace of these. The purpose of this study is to identify and map the major lineaments present in the Chitrial area and to establish their systematic pattern of development with the aid of the satellite images. Therefore, manual methods were applied to extract lineaments from satellite images in GIS platform. Figure 4.1a shows the lineament map of the total number of lineaments present in the area and its frequency distribution shown in figure 4.1b. To evaluate the fractures analyses of IRSP6 LISS III imagery data, the GIS technique has been attempted. Digital lineament maps were prepared by extracting the

lineaments manually from imagery data in GIS platform. Linear Directional Mean (LDM) considering the all lineaments trend in the Chitrial area is calculated by the equation given below

$$\textbf{LDM}= arctan \frac{\sum_{i=1}^{n} \sin \theta i}{\sum_{i=1}^{n} \cos \theta i}$$

where θi is the direction of a lineament present in the study area. The Linear directional mean of the Chitrial area shows an azimuth of 142°- 322°, i.e., a dominant NW – SE trend.

Lineament density analysis is applied to calculate the frequency of the lineaments per unit area; this map can be produced based on counting the pixels of line elements in a small window and assigning these values to the center pixel in the window in true geographic coordinates (Koike et al., 1995). Lineament density maps for the study area show the concentrations of lineaments over the entire area and the density of lineaments dominantly increased near the main mineralized block (Fig. 4.1b) of the Chitrial area. The faults can be distinguished from the map which extends mainly in NW-SE, N-S, WNW – ESE directions with a subordinate fault set extending in the NE-SW direction. Near the main block, lineaments are observed to be trending dominantly in a WNW – ESE direction. Analysis of lineaments are also undertaken from prepared lineament maps with the help of geostatistical analyst tool by which histograms are plotted to estimate variation in fracture density surrounding the main block and adjacent blocks within the basement granitoid (Figs 4.2a – 4.2c). From the lineament maps, orientation of the individual lineaments are also measured and combined to plot in

individual rose diagrams with angles ranging from 1to180 degrees (Chopra et al., 2009). These rose diagrams are used to analyze the distribution of lineaments based on the contribution of its frequency to the orientation trend. Rose diagrams were generated by counting each line as an element, despite its length being short or long. The process was accomplished with the help of the polar plot in the GIS platform. Figures 4.2d, 4.2e represent the rose diagrams of measured lineation data the main block, and block 1 respectively. Rose diagrams of identified lineaments and digitized faults are noticed to have developed in five principal directions (NW-SE, WNW – ESE, N-S, NE-SW, and E-W), the most dominant trends being the WNW – ESE and NW-SE trends. The dominant WNW-ESE trending lineament trend can be related to the Dindi lineament, which forms a major fault system in the Chitrial area. The orientations of major observed lineaments near the main block also show dominant trends in the WNW – ESE direction with azimuth ranging approximately 290°-330°.

4.3. Field structures

The basement granitoids are highly fractured (Fig. 4.3a) at most of the places. A large part of the basement surrounding Chitrial was subjected to rigorous fracture analysis as fractures in basement granitoids are not uniformly developed; rather they show variation in development depending upon both composition and intensity of deformation. It is observed that there are five prominent fracture sets present in the area which trend in the N-S, E - W, NNE-SSW and WNW-ESE directions. Two successive phases of brittle deformations (D4-D5) have been interpreted to have produced the observed fracture volume

within the grantoid rocks of the Chitrial area (Das et al., 2018). The D4 stage conjugate shear fracture development is restricted to the granitoids and gneisses of the area (Fig. 4.3b) while the D5 stage brittle event affects both the basement rocks as well as the overlying cover rocks of the Srisailam Formation. The D4 stage conjugate fractures are mainly shear fractures (Figs. 4.3c) with changing orientations over the study area. Systematic variation in orientation and recorded mutual overprinting relationships (Figs. 4.3 d,e,f) amongst these fracture sets has been related to changing orientation of the principal stress axes during the D4 stage and their later frequent reactivation during the D5 brittle event (Das et al., 2018). The Dindi lineament is interpreted to be one such D5 stage megascopic fault structure that displaces the basement granitoid - Srisailam Formation unconformity surface in an apparent dextral sense. D5 stage N-S, E-W, NE-SW and WNW-ESE trending faults are locally common in mesoscale within the sandstone outcrops. Effect of this later D5 stage faulting event is also pronounced within the sandstone outcrops with steepening and sudden changes in bedding orientations as well as fracture plane development.

Apart from fracture orientation data, fracture density was also measured from 2m × 2m blocks in suitable locations over the entire study area. A careful attempt was made to estimate the variation in fracture density within the basement granitoid with respect to the mineralized blocks as established by the AMD. AMD has already sub-divided the Chitrial area into several blocks, e.g., the Main Block, Block-1, Block-2, Block-3, and Block-4 according to uranium concentration

amongst which the Main Block hosts the actual uranium reserve of the area. With this view in mind, an attempt was made in the present study to estimate the number of fractures present in all possible locations in 2m X 2m grids around the main block as well as the other blocks. Fracture density in individual locations in blocks was thus tabulated. After calculating the total number of fracture present in 2mX2m grid within each block, the measured data of all the blocks were plotted in histograms (Fig. 4.4). From comparing the histogram for every individual blocks it is inferred that the fracture density is highest in the Main Block. With increasing distances from the centre of the Main Block, the fracture density also shows a sharp decrease. The measured counts indicate that the average fracture density is 35 – 50 /m^2 for the Main Block which is much higher in comparison to that measured from the adjoining 'Block 1 & 2' (10 – 25/m^2) and 'Block 4' (10 – 15/m^2). This is also supported by the digital lineament mapping. Combining the field data with satellite imagery data it can be concluded that the fracture density is inversely proportional with the distance from the Main Block. Rose diagrams which are made by using polar plots in GIS platform (Figs. 4.2d, 4.2e) indicates the main fracture trend in the mineralized Main block is NW-SE which is in confirmation with respect to the grid-wise fracture count data collected from the area. Histograms plotted using geostatistical analyst tool (Figs 4.2a – 4.2c) depicting fracture intensity indicates the number of fractures present per unit area is higher surrounding the mineralized Main Block compared to the other blocks. Again analysis of fractures using special statistical tool indicate that the Mean lineament trend of the fracture set to be WNW-ESE (142°).

4.4. Structural synthesis

Thus, both the techniques of using mesoscopic structural data and data obtained from imageries utilizing the GIS technique bears a good correlation and point towards a general increase in fracture population surrounding the mineralized Main Block with the dominant fracture trend in the mineralized zone being WNW-ESE to NW-SE. Keeping in mind the very important roles that fractures play either as direct pathways for ore-bearing fluids or channels for circulation of basinal brines that eventually concentrate the ore minerals scavenging the host basement near the developing unconformity surfaces, establishment of a near one-to-one relationship between increase in rock-fracture volume and the established uranium deposit becomes significant. It indicates that the increased fracture volume in the basement rocks directly or indirectly controlled ore mineralization in the Chitrial area with the WNW-ESE to NW-SE fracture set probably playing an active role behind mineralization.

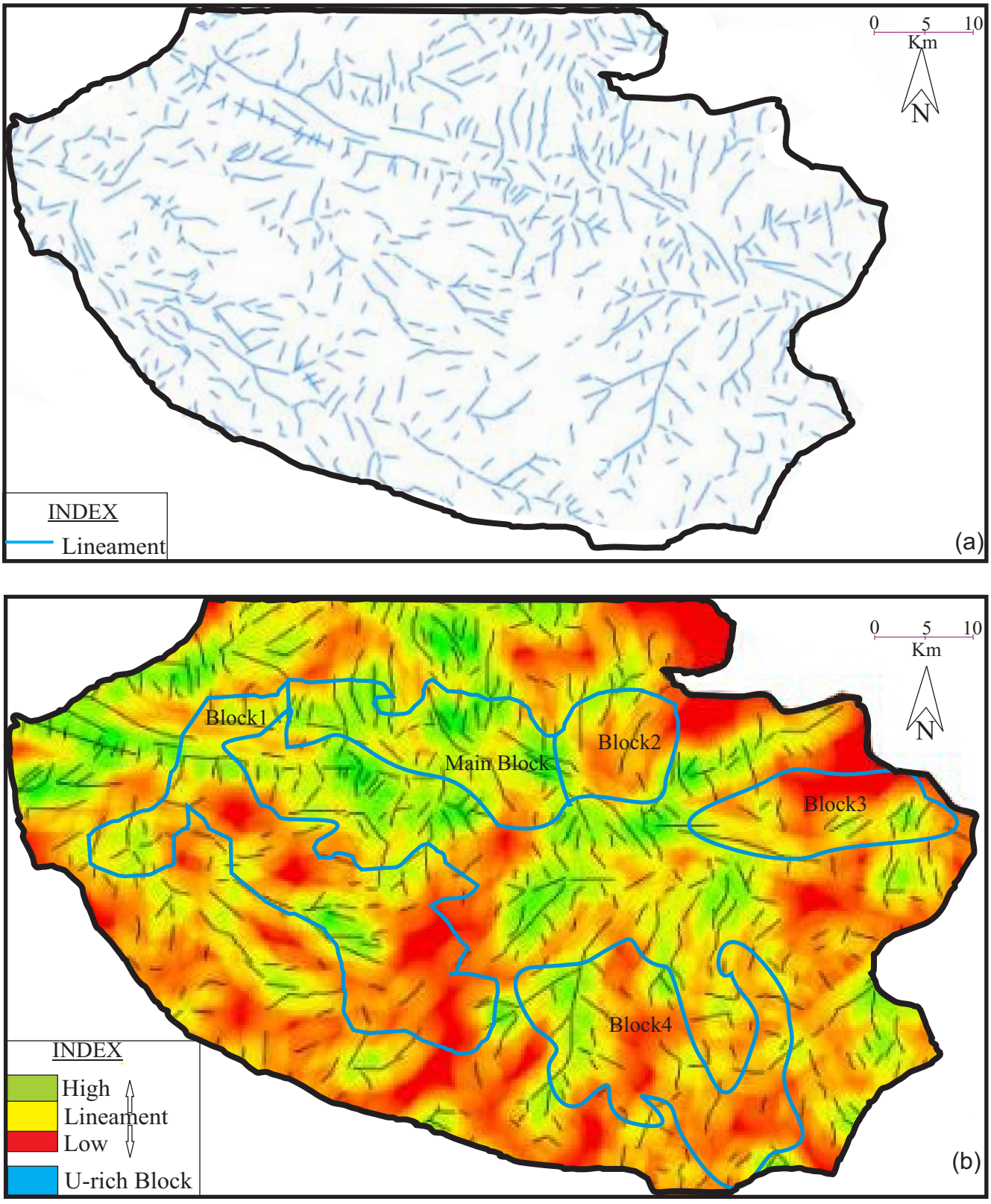

Figure. 4.1: (a) Lineament map with the total number of lineaments and its frequency distribution. Lineaments extracted from color composite satellite image. (b) Density map of lineament map with the uranium enriched block

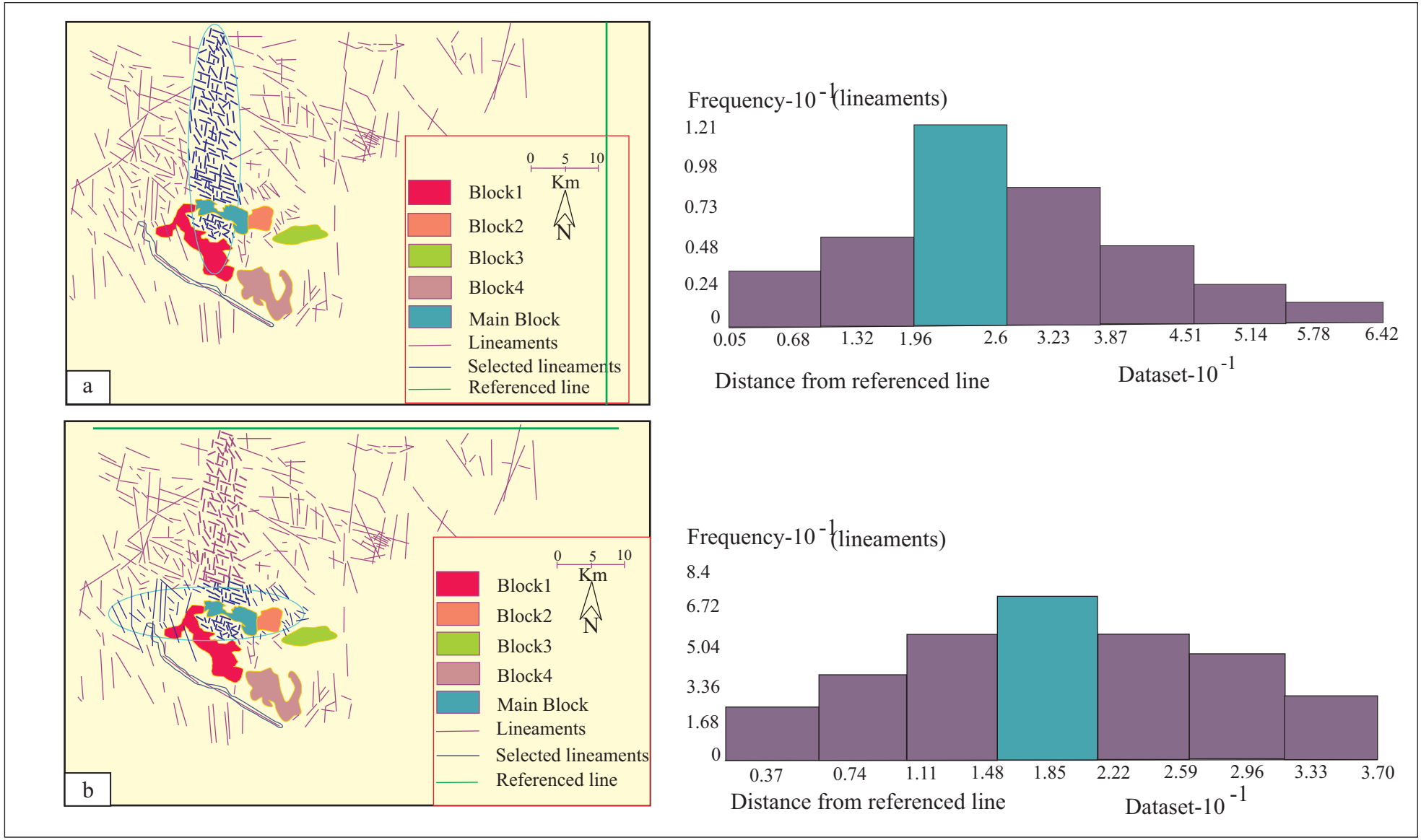

Figure 4.2: Histogram showing fracture frequency is higher near main block when plotted against the measured distance from east (a) and north (b) reference line respectively in GIS platform. blue ellipse marks the selected lineaments for highest pick in histogram.

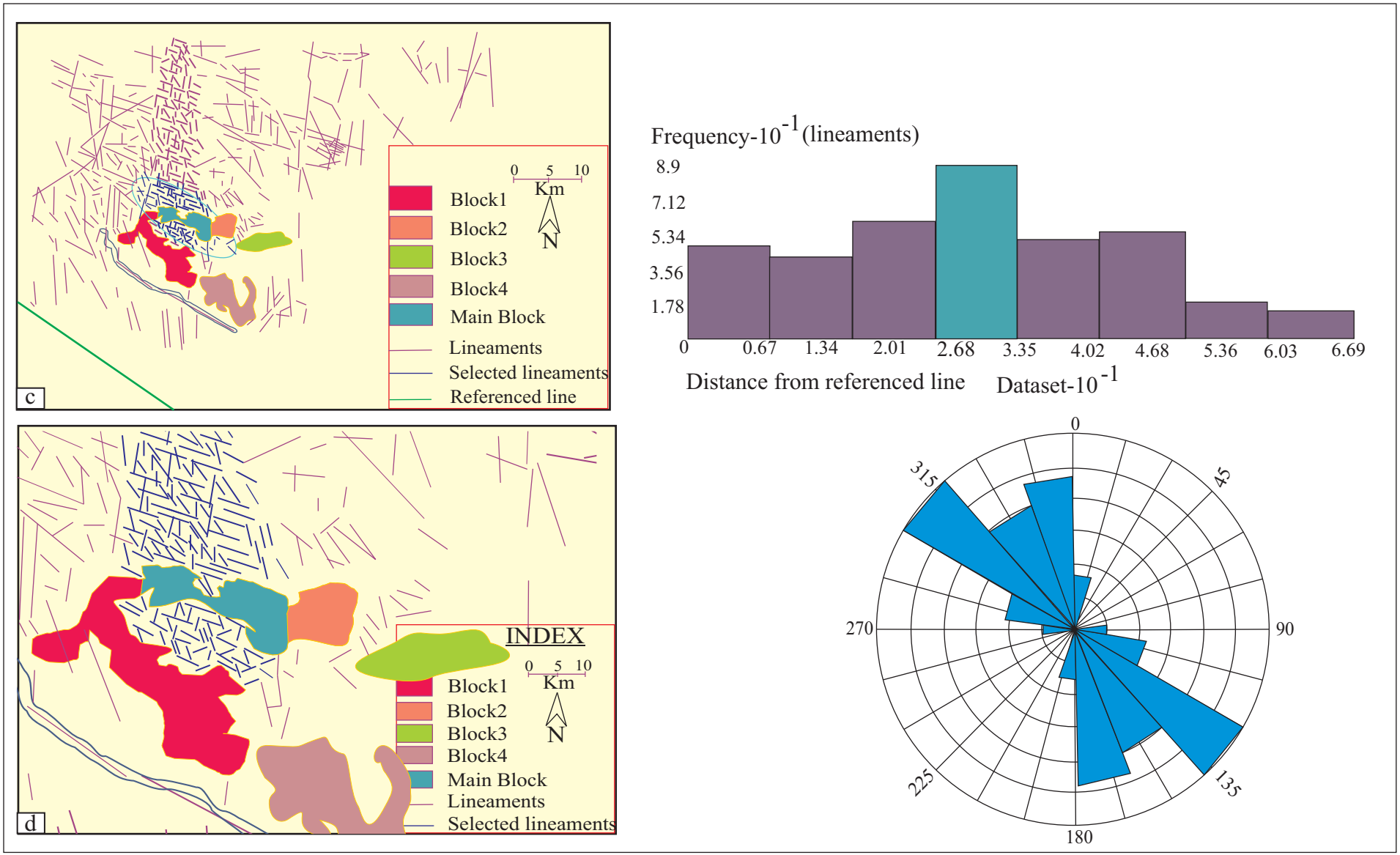

Figure 4.2: (c) Histogram showing fracture frequency is higher near main block when plotted against the measured distance from north west reference line in GIS platform. blue ellipse marks the selected lineaments for highest pick in histogram. (d) GIS map shows the selected lineaments (Left side) near main block and rose diagram represents the dominant trend of selected lineaments (right side).

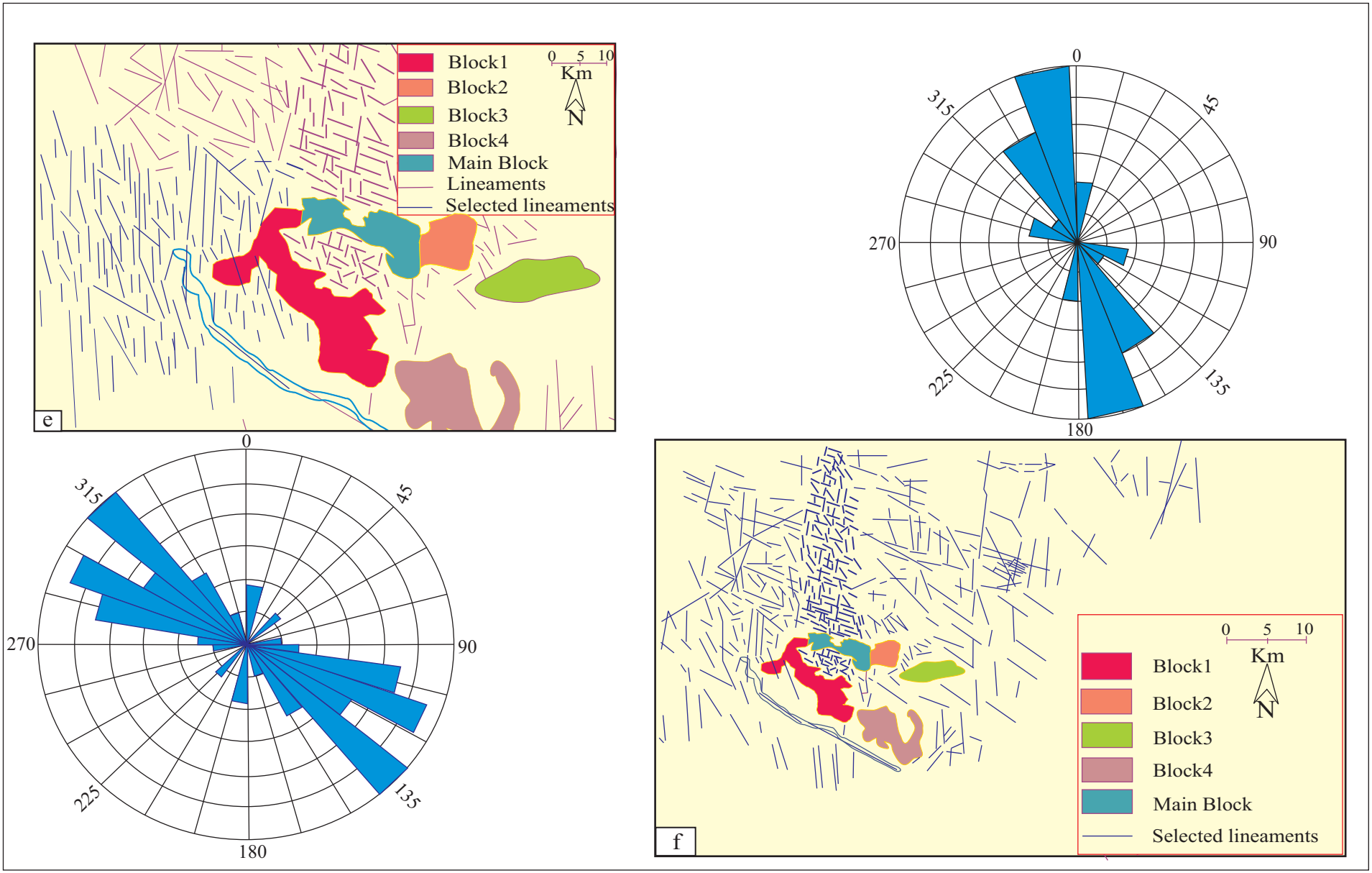

Figure 4.2: (e) GIS map shows the selected lineaments (Left side) near western part of block 1 and rose diagram represents the dominant trend of selected lineaments (right side). (f) Rose diagram represents the dominant trend of lineaments (left side) considering all the lineaments presents in the Chitrial area (Right side).

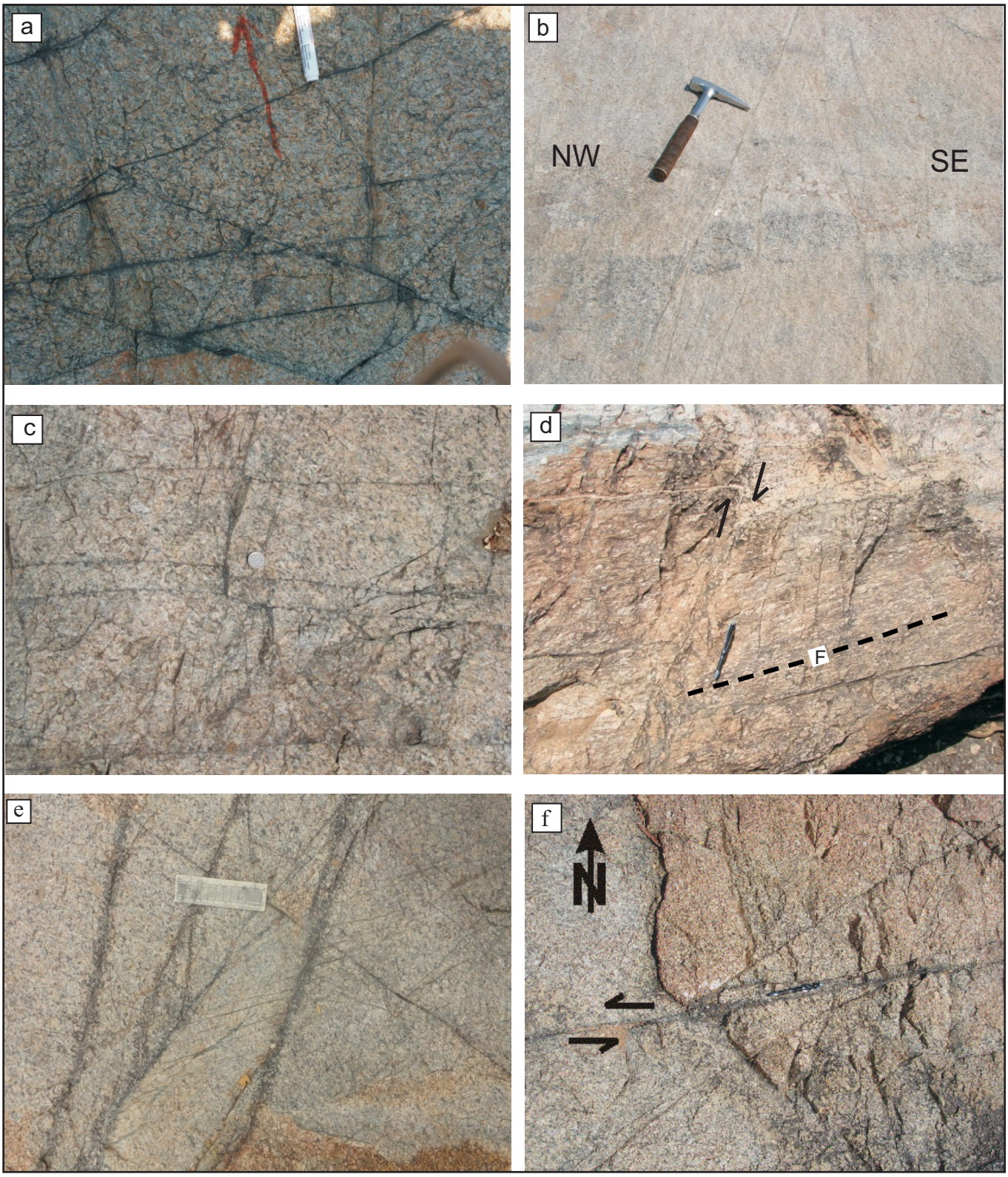

Figure 4.3: (a) Highly fractured granitoids; (b), (c) Development of conjugate shear fracture displacing early fabric within granite gneisses; (d), (e), (f) crosscutting relationship among the fracture sets within granitoids.

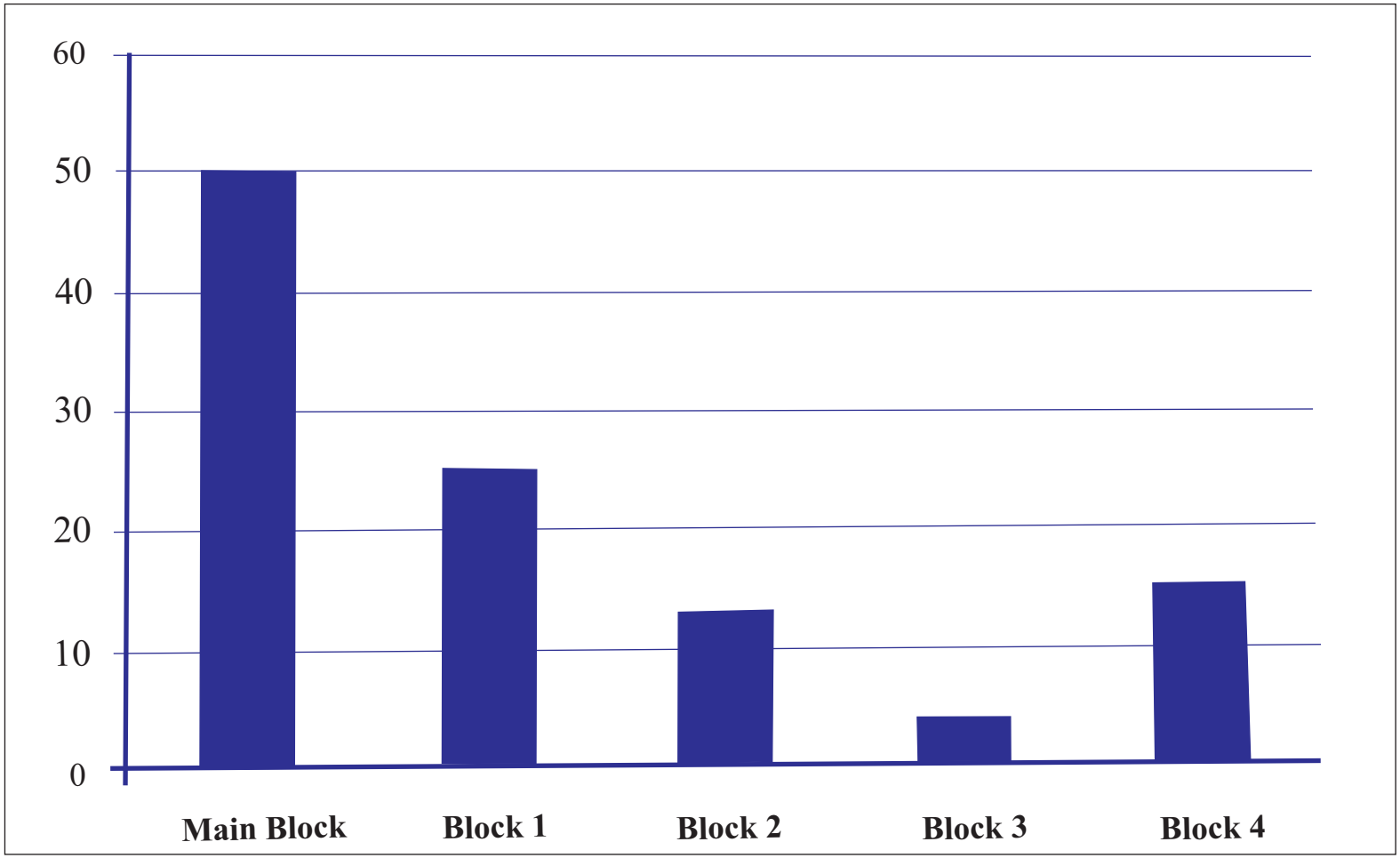

Figure 4.4: Histogram represents the average fracture density of each block (data collected from 2mx2m grid from field outcrop) in Chitrial area.